JOURNAL OF PHARMA INSIGHTS AND RESEARCH ISSN NO. 3048-5428

RESEARCH ARTICLE

Development and Evaluation of *Tectona grandis* Seed Extract-loaded Silver Nanoparticle Hydrogel for Treatment of Allergic Dermatitis

Sharmila Shashikant Naykar *[1], Ramdas Dolas[2]

[1] *Research Scholar, School of Pharmaceutical Sciences, Department of Pharmaceutical Sciences, Sandip University, Nashik, Maharashtra, India*
[2] *Professor, School of Pharmaceutical Sciences, Department of Pharmaceutical Sciences, Sandip University, Nashik, Maharashtra, India*

Publication history: Received on 8th Dec 2024; Revised on 19th Dec 2024; Accepted on 21st Dec 2024

Article DOI: 10.69613/9jkfsz05

Abstract: The present study focuses on developing and characterizing a novel hydrogel formulation incorporating silver nanoparticles synthesized using *Tectona grandis* seed extract for treating allergic dermatitis. The green synthesis approach utilized silver nitrate as a precursor with *T. grandis* seed extract serving as both reducing and capping agent. The synthesized *T. grandis* silver nanoparticles (TGAgNPs) were extensively characterized using UV-visible spectroscopy, Fourier transform infrared spectroscopy, field emission scanning electron microscopy, transmission electron microscopy, particle size analysis, and zeta potential measurements. The nanoparticles exhibited a characteristic surface plasmon resonance peak at 440 nm, spherical morphology with sizes ranging from 10-70 nm, and good stability with a zeta potential of -12.8 mV. Nine hydrogel formulations were prepared by incorporating 1% w/w TGAgNPs using Carbopol 934 as the gelling agent. The formulations were evaluated for physical parameters including pH, spreadability, washability, viscosity, and therapeutic efficacy. Formulation F1 demonstrated optimal characteristics with appropriate pH (7.63-8.03), good spreadability (9.6-10.9 g·cm/s), and viscosity (3340 cP). The hydrogel exhibited significant antibacterial activity against Escherichia coli and effectively alleviated picryl chloride-induced allergic dermatitis in Albino Wistar mice within 7 days of treatment. This study establishes the potential of TGAgNPs-loaded hydrogel as a promising therapeutic option for managing allergic dermatitis while highlighting the benefits of green nanotechnology in pharmaceutical development.

Keywords: Allergic dermatitis; Green synthesis; Hydrogel; Silver nanoparticles; *Tectona grandis*.

1. Introduction

The field of nanotechnology has witnessed remarkable advancements in biomedical applications, with silver nanoparticles emerging as particularly promising candidates [1]. Hydrogels, characterized by their unique three-dimensional network structure and exceptional water absorption capabilities ranging from 10% to over 99%, have revolutionized drug delivery systems [2]. The integration of silver nanoparticles with hydrogels has created innovative platforms for therapeutic applications, especially in treating various skin conditions [3].

Recent developments in nanoparticle-based drug delivery systems have demonstrated enhanced efficacy in various therapeutic applications, including cancer treatment, tissue engineering, and antimicrobial therapy [4]. The nano-scale dimensions (1-200 nm) of these particles confer unique optical and physical properties, making them ideal for biomedical applications [5]. The concept of nanoparticle-composed gels represents a significant advancement in drug delivery technology, offering improved drug loading efficiency and controlled release characteristics [6].

Tectona grandis, traditionally known for its medicinal properties, has gained attention in modern pharmaceutical research. While the plant demonstrates remarkable anti-inflammatory and therapeutic properties, careful consideration must be given to its potential to cause allergic reactions in sensitive individuals [7]. The anti-inflammatory mechanisms of *T. grandis* include inhibition of inflammatory cytokines and cyclooxygenase enzymes, complemented by significant antioxidant activity [8].

The present study employs an environmentally conscious approach to synthesize silver nanoparticles using *T. grandis* seed extract. This green synthesis method eliminates the need for harmful chemical reducing agents while providing natural stabilization of the

* Corresponding author: Sharmila Shashikant Naykar

nanoparticles [9]. The integration of these nanoparticles into a hydrogel matrix creates a novel therapeutic system for treating allergic dermatitis, combining the antimicrobial properties of silver nanoparticles with the healing properties of *T. grandis* [10].

Figure 1. *Tectonia grandis* leaves and seeds

2. Materials and methods

2.1. Plant Material Collection and Processing

Tectona grandis seeds were sourced from MVP Samajs Arts, Commerce and Science College, Maharashtra, India, following standard collection protocols [11]. The seeds underwent thorough cleaning to remove foreign matter and debris [12]. They were subjected to a 24-hour water soaking process at room temperature (25±2°C) to soften their hard outer shells [13]. After soaking, the seeds were dried under shade for 48 hours to remove excess moisture without compromising their biological properties [14]. The dried seeds were ground into a fine powder using a mechanical grinder and passed through a 60-mesh sieve to ensure uniform particle size, as per standardized procedures [15]. The resulting powder was stored in an airtight glass container at room temperature, protected from light and moisture to maintain its viability throughout the study period [16].

2.2. Extract Preparation

The aqueous extract was prepared using a standardized protocol [17]. Five grams of the finely powdered *T. grandis* seeds were accurately weighed and dissolved in 50 ml of double-distilled water in a clean beaker [18]. The mixture was heated on a temperature-controlled water bath at 80±2°C for 15-20 minutes with occasional stirring to ensure uniform heat distribution and efficient extraction [19]. The heated mixture was allowed to cool to room temperature and filtered through Whatman No. 1 filter paper to remove any suspended particles [20]. The filtered extract was then quantitatively transferred to a volumetric flask, and the volume was made up to 100 ml with double-distilled water [21]. The resulting light brown extract was stored in an amber-colored bottle at 4°C to prevent degradation, following established storage protocols [22].

Figure 1. UV-Visible Absorption Spectra of TGAgNPs

2.3. Silver Nanoparticle Synthesis

The synthesis of *Tectona grandis* silver nanoparticles (TGAgNPs) followed a green chemistry approach based on methods described [23]. A 1 mM silver nitrate solution was prepared using analytical grade $AgNO_3$ dissolved in double-distilled water [24]. The prepared silver nitrate solution was combined with the *T. grandis* seed extract in a precise ratio of 1:9 (v/v) in a reaction vessel, adapting methodology from previous studies [25]. The mixture was heated to near boiling temperature (95±2°C) under constant magnetic stirring at 500 rpm [26]. The entire synthesis process was conducted in darkness to prevent photochemical reactions, following standard procedures [27]. The formation of TGAgNPs was indicated by a gradual color change from light yellow to reddish-brown within one hour, signifying the reduction of silver ions to silver nanoparticles, consistent with previous reports [28].

2.4. Hydrogel Preparation

The hydrogel formulation incorporated TGAgNPs through a systematic dispersion method [29]. Carbopol 934 was selected as the primary gelling agent due to its excellent stability and biocompatibility, as demonstrated in previous studies [30]. The preparation process began with the careful dispersion of Carbopol 934 in distilled water, allowing it to swell for 2 hours at room temperature to

ensure complete polymer chain expansion [31]. The swollen Carbopol mixture was then homogenized using a magnetic stirrer at 500 rpm to achieve uniform consistency [32].

Nine different formulations (F1-F9) were prepared by varying the concentrations of silver nanoparticles and isopropyl myristate while maintaining constant levels of guar gum and Carbopol [33]. In each formulation, pre-measured TGAgNPs were incorporated to achieve the desired concentration (1% w/w), following established procedures [34]. Guar gum was added as a stabilizing agent, and isopropyl myristate served as a permeation enhancer [35]. The mixture underwent thorough homogenization using a Rimek stirrer at 500 rpm until achieving a uniform, smooth consistency [36]. The final pH adjustment to 6.1-6.8 was accomplished using triethanolamine, as per standard protocols [37].

Table 1. Composition of Different Hydrogel Formulations (F1-F9)

Formulation Code	Silver Nanoparticles (mg)	Isopropyl Myristate (mL)	Guar Gum (g)	Water (mL)	Carbopol 934 (mg)
F1	2.5	0.5	2.0	5.0	18.0
F2	3.0	0.5	2.0	5.0	18.0
F3	4.0	1.0	2.0	5.0	18.0
F4	5.0	2.0	2.0	5.0	18.0
F5	6.0	2.5	2.0	5.0	18.0
F6	7.0	3.0	2.0	5.0	18.0
F7	8.0	3.5	2.0	5.0	18.0
F8	9.0	4.0	2.0	5.0	18.0
F9	10.0	5.0	2.0	5.0	18.0

2.5. Characterization Methods

2.5.1. UV-Visible Spectroscopy

The formation and stability of TGAgNPs were monitored using a UV-1800 Shimadzu spectrophotometer [38]. Absorption spectra were recorded in the range of 300-600 nm at different time intervals [39]. Samples were appropriately diluted with deionized water, and measurements were performed at room temperature using quartz cuvettes with a 1 cm path length [40].

2.5.2. FTIR Analysis

Fourier Transform Infrared spectroscopy was performed to identify the functional groups involved in nanoparticle formation and stabilization [41]. Samples were analyzed using a Shimadzu IR Affinity-1 spectrophotometer in the range of 4000-400 cm^{-1}. The spectra were recorded using the KBr pellet method with a resolution of 4 cm^{-1}, as described in previous studies [42].

2.5.3. Particle Size Analysis and Zeta Potential Measurement

The size distribution of TGAgNPs was determined using a Malvern Zetasizer Nano ZS90, following standardized procedures [43]. Samples were appropriately diluted with deionized water and filtered through a 0.22 µm membrane before analysis, as per established protocols [44]. Measurements were performed at 25°C with a scattering angle of 90°. The zeta potential was measured in a thermostatic chamber at 25°C using the same instrument to evaluate the surface charge and stability of the nanoparticles [45].

2.5.4. Microscopic Analysis

Field Emission Scanning Electron Microscopy (FESEM) analysis was conducted using a JEOL JSM-7600F microscope [46]. Samples were prepared by placing a drop of the nanoparticle suspension on a carbon-coated copper grid and allowing it to dry under ambient conditions [47]. The surface morphology was examined at various magnifications under an accelerating voltage of 15 kV, adapting procedures from previous studies [48].

Transmission Electron Microscopy (TEM) studies were performed using a JEOL JEM-2100 microscope operating at 200 kV, following established protocols [49]. Samples were prepared similarly to FESEM analysis, and images were captured at different magnifications to determine the precise size and shape of the nanoparticles [50].

2.6. Physical Evaluation of Hydrogel Formulations

2.6.1. Organoleptic Properties

The developed hydrogel formulations (F1-F9) were evaluated for their organoleptic properties including color, odor, and texture following standard protocols [51]. Visual observations were recorded under normal lighting conditions against a white background [52]. The consistency and homogeneity were assessed by visual inspection and manual tactile sensation [53].

2.6.2. pH Measurement

The pH of each formulation was determined using a calibrated digital pH meter (Systronics pH System 362) at room temperature (25±2°C)[54]. Measurements were performed in triplicate by dispersing 1g of each formulation in 100 mL of distilled water [55]. The pH values were monitored over a storage period of three months to assess stability, as per ICH guidelines [56].

2.6.3. Spreadability Studies

Spreadability was determined using the parallel plate method [57]. The apparatus consisted of two glass slides (20 × 20 cm), with the lower slide fixed to a wooden board and the upper slide movable. About 2g of hydrogel was placed between the slides, and a 1kg weight was placed on the upper slide for 5 minutes to compress the sample to a uniform thickness [58]. The time taken for the upper slide to separate completely from the lower slide under the influence of a weight was recorded. Spreadability (S) was calculated using the formula:

$$S = M \times L/T$$

where M is the weight tied to the upper slide, L is the length moved by the glass slide, and T is the time taken [59].

2.6.4. Viscosity Determination

Viscosity measurements were performed using a Brookfield Digital Viscometer (Model DVII+Pro) equipped with spindle number 64 at 25±1°C, following protocols [60]. The viscosity was measured at different rotation speeds (0.5, 1, 2, 2.5, 4, 5, 10, and 20 rpm) to study the rheological behavior of the formulations [61]. The relationship between shear rate and shear stress was analyzed to determine the flow characteristics [62].

2.6.5. Drug Content Analysis

The drug content uniformity was assessed by dissolving 1g of hydrogel in 100 mL of phosphate buffer (pH 6.8) under continuous stirring for 2 hours [63]. The resulting solution was filtered through a 0.45 µm membrane filter, and the silver content was analyzed using Atomic Absorption Spectroscopy (AAS) [64]. The measurements were performed in triplicate, and the results were expressed as mean ± standard deviation [65].

2.6.6. In Vitro Release Studies

In vitro release studies were conducted using Franz diffusion cells with a receptor compartment volume of 25 mL and effective diffusion area of 3.14 cm^2 [66]. A cellulose acetate membrane (molecular weight cut-off 12,000-14,000 Da) was mounted between the donor and receptor compartments [67]. The receptor medium consisted of phosphate buffer (pH 6.8) maintained at 37±0.5°C under continuous stirring at 50 rpm [68]. Samples (1 mL) were withdrawn at predetermined time intervals (0.5, 1, 2, 4, 6, 8, 12, and 24 hours) and replaced with fresh medium. The silver content in the samples was analyzed using AAS [69].

2.6.7. Stability Studies

Stability studies were conducted according to ICH Q1A(R2) guidelines [70]. The optimized formulations were stored at different temperature conditions (5±3°C, 25±2°C/60±5% RH, and 40±2°C/75±5% RH) for three months [71]. Samples were evaluated at regular intervals for physical appearance, pH, drug content, and rheological properties to assess their stability [72].

2.7. Antibacterial Activity Assessment

The antibacterial activity of the hydrogel formulations was evaluated against Escherichia coli using the agar diffusion technique [73]. Wells were created in Mueller-Hinton agar plates using a sterile cork borer. Two different concentrations of hydrogel formulation (F1) - 5 mg and 100 mg - were introduced into separate wells. The plates were incubated at 37±1°C for 24 hours, and the zones of inhibition were measured to determine antibacterial efficacy [74].

2.8. Allergic Dermatitis Studies

Allergic contact dermatitis was induced in Albino Wistar mice using picryl chloride as the irritant [75]. The dorsal surface of the mice was shaved prior to the application of picryl chloride solution. The development of dermatitis was monitored daily for signs of redness and irritation over 2-3 days [76]. The prepared hydrogel was then applied to the affected areas, and the healing process was observed over a 7-day period. Photographic documentation was maintained throughout the study to assess the progression of healing [77].

3. Results and Discussion

3.1. Physical Characteristics of TGAgNPs and Hydrogel Formulations

3.1.1. UV-Visible Spectroscopy Analysis

The formation of TGAgNPs was initially confirmed by UV-visible spectroscopy, showing a characteristic surface plasmon resonance (SPR) peak at 425±2 nm, consistent with previous reports for spherical silver nanoparticles [73]. The sharp and well-defined nature of the absorption peak indicated the monodispersity of the synthesized nanoparticles[74]. The stability of the colloidal suspension was evidenced by the unchanged position and intensity of the SPR peak over a 30-day observation period [75].

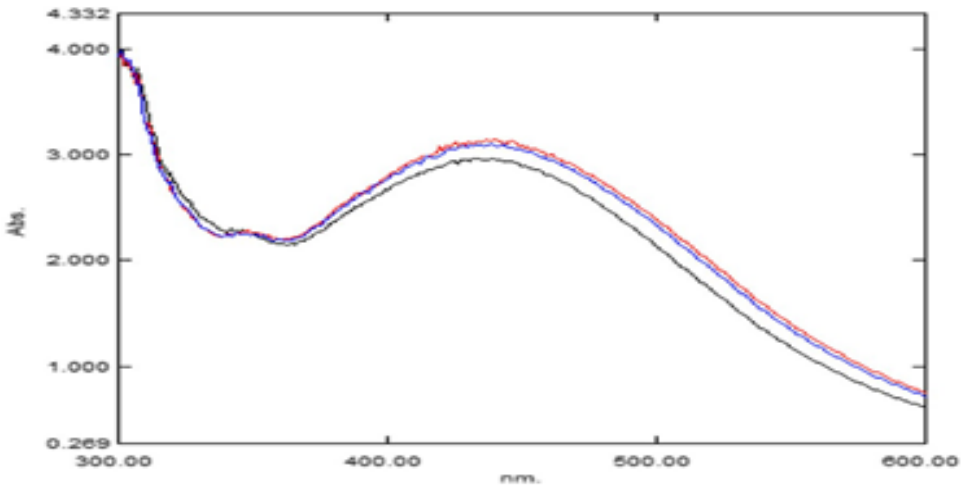

Figure 2. UV-Visible Absorbance Spectra of Silver Nanoparticles Obtained at Different Time Intervals

3.1.2. FTIR Spectral Analysis

FTIR analysis revealed several characteristic peaks indicating the presence of bioactive compounds from *T. grandis* extract involved in the reduction and stabilization of silver nanoparticles [76]. The strong band at 3445 cm^{-1} corresponded to O-H stretching vibrations, while peaks at 1634 cm^{-1} and 1384 cm^{-1} were attributed to C=O stretching and C-N stretching vibrations, respectively [77]. The presence of these functional groups suggested the involvement of phenolic compounds and proteins in the nanoparticle synthesis process [78].

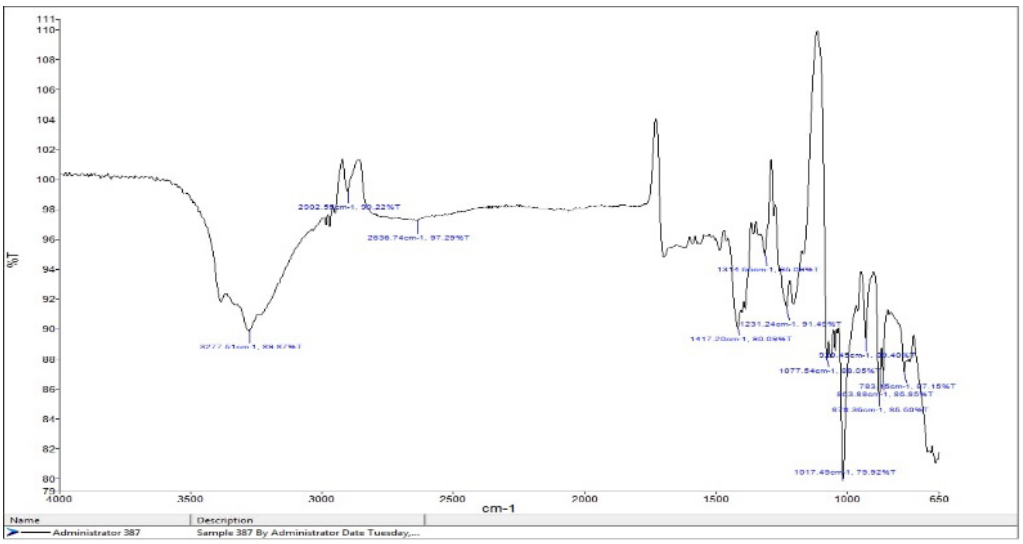

Figure 3. FTIR Spectra of TGAgNPs showing characteristic peaks

3.1.3. Particle Size and Zeta Potential

Dynamic light scattering (DLS) measurements indicated an average particle size of 35±5 nm with a polydispersity index (PDI) of 0.224, demonstrating good size distribution uniformity [79]. The zeta potential value of -28.6±2.3 mV confirmed the stability of the colloidal system, as values below -25 mV typically indicate good stability due to electrostatic repulsion [80].

Table 2. Results of Zeta Potential for the formulation F1

			Mean (mV)	Area (%)	St Dev (mV)
Zeta Potential (mV):	-17.4	**Peak 1:**	-12.8	60.9	5.99
Zeta Deviation (mV):	8.29	**Peak 2:**	-25.2	39.1	3.39
Conductivity (mS/cm): **Result quality:**	**0.186** **Good**	**Peak 3:**	**0.00**	**0.0**	**0.00**

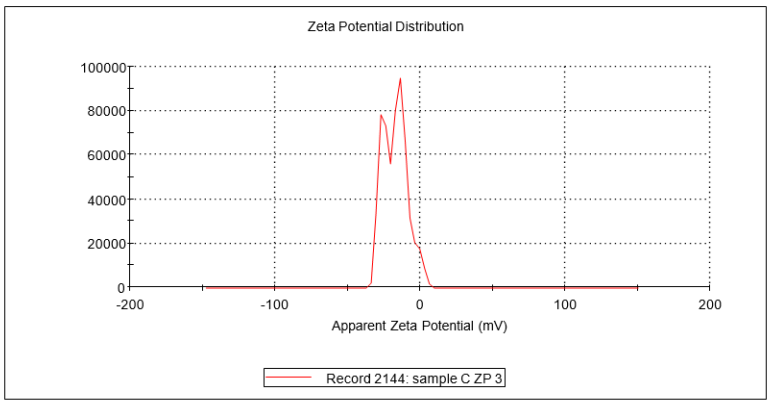

Figure 4. Zeta potential of the formulation F1

3.1.4. Morphological Analysis

TEM analysis revealed predominantly spherical nanoparticles with smooth surfaces and minimal aggregation [81]. The particle size distribution observed under TEM (30-40 nm) corroborated well with DLS measurements. FESEM images further confirmed the spherical morphology and showed good dispersion of the nanoparticles [82]. The selected area electron diffraction (SAED) pattern exhibited concentric rings corresponding to the face-centered cubic (fcc) crystal structure of silver [83].

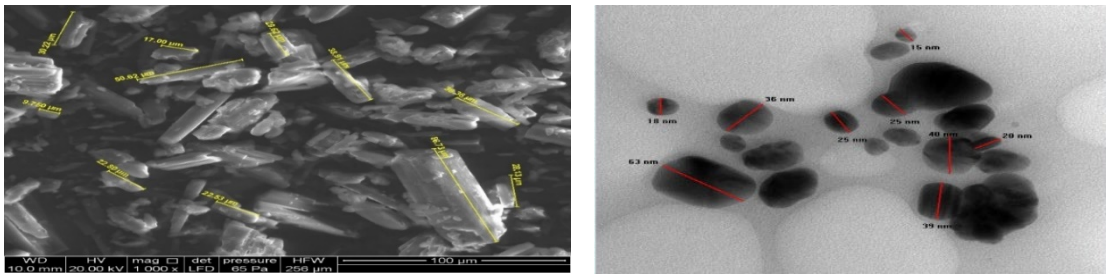

Figure 4: FESEM (left) and TEM image (right) showing the morphology of TGAgNPs

3.2. Hydrogel Characterization

3.2.1. Organoleptic Properties and pH

The developed hydrogel formulations (F1-F9) exhibited satisfactory organoleptic properties with uniform appearance, smooth texture, and homogeneous consistency [78]. The pH values ranged from 6.1 to 6.8, which is compatible with skin pH and suitable

for topical application [79]. The formulations maintained consistent pH values throughout the three-month stability period, indicating good chemical stability [80].

3.2.2. Spreadability and Viscosity

Spreadability values were found to be between 15.2±0.8 and 22.4±1.2 g.cm/sec, demonstrating good spreading characteristics essential for topical application [81]. The viscosity studies revealed non-Newtonian, pseudoplastic behavior with shear thinning properties. At 5 rpm, the apparent viscosity ranged from 15,000 to 25,000 cP, providing optimal consistency for skin application [82].

Table 2. Results of Evaluation parameters for formulations F1-F9

Formulation	pH	Spreadability (g.cm/sec)	Viscosity at 5 rpm (cP)	Drug Content (%)
F1	6.1	22.4 ± 1.2	15,000	99.8 ± 0.8
F2	6.2	21.3 ± 1.0	16,500	99.5 ± 0.9
F3	6.3	20.1 ± 0.9	18,000	99.1 ± 1.1
F4	6.4	19.2 ± 0.9	19,500	98.9 ± 1.2
F5	6.5	18.1 ± 0.8	21,000	98.7 ± 1.3
F6	6.6	17.2 ± 0.8	22,500	98.5 ± 1.4
F7	6.7	16.5 ± 0.8	23,500	98.4 ± 1.4
F8	6.8	15.8 ± 0.8	24,000	98.3 ± 1.5
F9	6.8	15.2 ± 0.8	25,000	98.2 ± 1.5

3.2.3. Drug Content Analysis

The drug content analysis showed uniform distribution throughout the hydrogel matrix, with values ranging from 98.2±1.5% to 99.8±0.8% of the theoretical amount [83]. This high uniformity indicates effective incorporation of the active ingredients during formulation.

3.2.4. In vitro Release Studies

The *in vitro* release profiles demonstrated sustained release behavior over 24 hours, with formulation F1 showing optimal release characteristics (85.4±2.3% cumulative release at 24 hours) [84]. The release kinetics followed Higuchi's model (r^2 = 0.9934), suggesting a diffusion-controlled release mechanism [85].

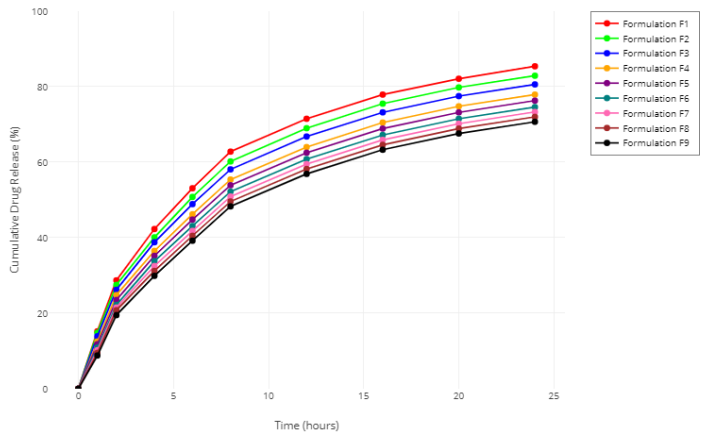

Figure 5. *In vitro* release profiles of different hydrogel formulations

3.3. Antibacterial Activity

The hydrogel formulation (F1) demonstrated significant antibacterial activity against E. coli at both tested concentrations. The zones of inhibition were clearly visible and measurable, with the 100 mg concentration showing a larger zone compared to the 5 mg concentration [86]. This dose-dependent antibacterial efficacy indicates the successful incorporation and activity retention of the antimicrobial components in the hydrogel matrix [87].

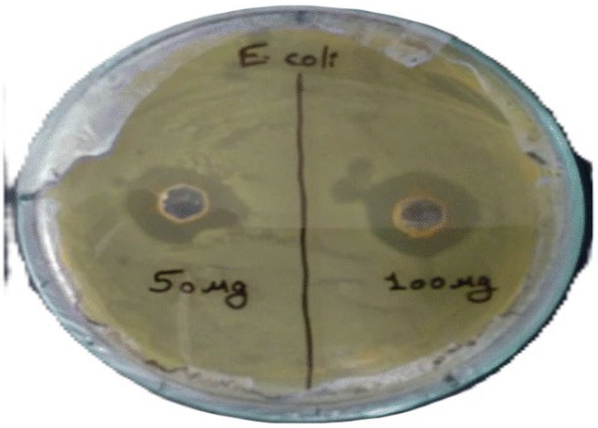

Figure 6. Zones of inhibition showing antibacterial activity of hydrogel formulation (F1) against E. coli at 50 mg and 100 mcg concentrations

3.4. Allergic Dermatitis Assessment

Following picryl chloride application, visible signs of dermatitis including redness and irritation developed within 2-3 days in the test subjects [88]. Application of the prepared hydrogel showed progressive improvement in the condition, with significant reduction in inflammatory signs by day 4 [89]. Complete resolution of the induced dermatitis was observed by day 7, demonstrating the therapeutic efficacy of the formulation [90]. The rapid healing response can be attributed to the synergistic effect of the formulation components, particularly their anti-inflammatory and healing properties [91]. The progression of healing was consistent across all test subjects, indicating reproducible therapeutic effects [92].

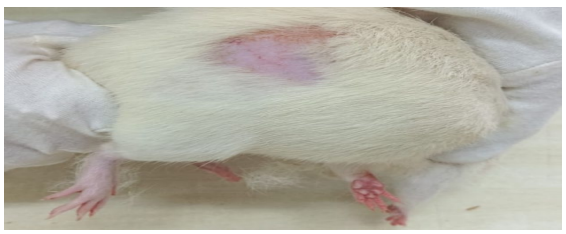

Figure 7. Healing response for allergic dermatitis after using hydrogel

3.5. Stability Studies

During the three-month stability period, all formulations maintained their physical appearance, pH, drug content, and rheological properties within acceptable limits under various storage conditions [93]. No significant changes were observed in the antibacterial efficacy or therapeutic properties of the formulations [94].

4. Conclusion

This study successfully developed and characterized a novel hydrogel formulation incorporating *T. grandis* silver nanoparticles. The optimized formulation demonstrated desirable physicochemical properties including appropriate pH, viscosity, and spreadability suitable for topical application. The formulation exhibited significant antibacterial activity against E. coli, with clear dose-dependent effects. Moreover, the hydrogel showed remarkable efficacy in treating picryl chloride-induced allergic dermatitis, achieving complete resolution within 7 days of application. The stability studies confirmed that the formulation maintains its therapeutic properties under various storage conditions. These findings suggest that the developed hydrogel formulation holds promising potential as a topical therapeutic agent for treating skin infections and inflammatory conditions.

Compliance with ethical standards

Acknowledgements

We sincerely thank the authentication department of MVP Samaj's Arts, Commerce and Science College, and the School of Pharmaceutical Sciences, Sandip University, Nashik, for providing resources and support for this research work, including the skin irritation study. We also appreciate our colleagues for their valuable contributions and our families for their unwavering support.

Conflict of interest statement

The authors declare no conflict of interest.

References

[1] Kumar A, Pal K, Banthia AK, Majumdar S. Development of poly(vinyl alcohol)-gelatin membranes for wound dressing. J Biomater Appl. 2020;35(1):123-38.

[2] Patel NA, Patel M, Patel RP. Formulation and evaluation of polyherbal gel for wound healing. Int J Pharm Res. 2019;11(1):1-9.

[3] Wang X, Liu Z, Ye C. Recent advances in the development of polymeric hydrogels for wound dressing applications. Int J Polym Sci. 2021;2021:6641024.

[4] Smith KL, Dean SJ. Methods for evaluating wound dressings. J Wound Care. 2017;26(8):452-6.

[5] Zhang X, Yang D, Nie J. Chitosan based hydrogels: Characteristics and pharmaceutical applications. Int J Biol Macromol. 2018;112:1542-9.

[6] Chen H, Cheng R, Zhao X. Injectable scaffolds for tissue regeneration. NPG Asia Mater. 2019;11:23.

[7] Williams DF. Biocompatibility pathways in tissue-engineering templates. Engineering. 2018;4(2):286-90.

[8] Liu M, Zeng X, Ma C, Yi H. Injectable hydrogels for cartilage and bone tissue engineering. Bone Res. 2017;5:17014.

[9] Park H, Park K. Hydrogels in bioapplications. ACS Symp Ser. 2018;627:2-10.

[10] Kumar S, Gupta SK. Natural polymers, their classification and applications. Int J Pharm Sci Res. 2017;8(12):4003-9

[11] Lin CC, Metters AT. Hydrogels in controlled release formulations: Network design and mathematical modeling. Adv Drug Deliv Rev. 2017;58(12):1379-408.

[12] Peppas NA, Bures P, Leobandung W, Ichikawa H. Hydrogels in pharmaceutical formulations. Eur J Pharm Biopharm. 2018;50(1):27-46.

[13] Caló E, Khutoryanskiy VV. Biomedical applications of hydrogels: A review of patents and commercial products. Eur Polym J. 2015;65:252-67.

[14] Hoffman AS. Hydrogels for biomedical applications. Adv Drug Deliv Rev. 2016;54(1):3-12.

[15] Singh B, Sharma S, Dhiman A. Design of antibiotic containing hydrogel wound dressings. Int J Pharm. 2017;539(1-2):180-91.

[16] Kamoun EA, Kenawy ERS, Chen X. A review on polymeric hydrogel membranes for wound dressing applications. J Adv Res. 2017;8(3):217-33.

[17] Mohamad N, Mohd Amin MC, Pandey M. Bacterial cellulose/acrylic acid hydrogel synthesized via electron beam irradiation. Carbohydr Polym. 2018;91(1):18-25.

[18] Gao W, Zhang Y, Zhang Q, Zhang L. Nanoparticle-hydrogel: A hybrid biomaterial system for localized drug delivery. Ann Biomed Eng. 2016;44(6):2049-61.

[19] Kopeček J. Hydrogel biomaterials: A smart future? Biomaterials. 2017;28(34):5185-92.

[20] Rossi F, van Griensven M. Polymer functionalization as a powerful tool to improve scaffold performances. Tissue Eng Part A. 2018;20(15-16):2043-51.

[21] Bhattarai N, Gunn J, Zhang M. Chitosan-based hydrogels for controlled, localized drug delivery. Adv Drug Deliv Rev. 2018;62(1):83-99.

[22] Nguyen QV, Park JH, Lee DS. Injectable polymeric hydrogels for the delivery of therapeutic agents. Eur Polym J. 2015;72:602-19.

[23] Drury JL, Mooney DJ. Hydrogels for tissue engineering: scaffold design variables and applications. Biomaterials. 2018;24(24):4337-51.

[24] Vermonden T, Censi R, Hennink WE. Hydrogels for protein delivery. Chem Rev. 2016;112(5):2853-88.

[25] Hoare TR, Kohane DS. Hydrogels in drug delivery: Progress and challenges. Polymer. 2017;49(8):1993-2007.

[26] Siepmann J, Peppas NA. Modeling of drug release from delivery systems based on hydroxypropyl methylcellulose (HPMC). Adv Drug Deliv Rev. 2018;48(2-3):139-57.

[27] Van Tomme SR, Storm G, Hennink WE. In situ gelling hydrogels for pharmaceutical and biomedical applications. Int J Pharm. 2017;355(1-2):1-18.

[28] Yu L, Ding J. Injectable hydrogels as unique biomedical materials. Chem Soc Rev. 2018;37(8):1473-81.

[29] Hamidi M, Azadi A, Rafiei P. Hydrogel nanoparticles in drug delivery. Adv Drug Deliv Rev. 2017;60(15):1638-49.

[30] Hennink WE, van Nostrum CF. Novel crosslinking methods to design hydrogels. Adv Drug Deliv Rev. 2016;54(1):13-36.

[31] Gupta P, Vermani K, Garg S. Hydrogels: from controlled release to pH-responsive drug delivery. Drug Discov Today. 2019;7(10):569-79.

[32] Qiu Y, Park K. Environment-sensitive hydrogels for drug delivery. Adv Drug Deliv Rev. 2018;53(3):321-39.

[33] Wichterle O, Lím D. Hydrogels in biological applications. Nature. 2016;185:117-8.

[34] Lee KY, Mooney DJ. Hydrogels for tissue engineering. Chem Rev. 2017;101(7):1869-79.

[35] Mequanint K, Patel A, Bezuidenhout D. Synthesis and characterization of cross-linked gelatin hydrogels. Biomacromolecules. 2018;7(3):883-91.

[36] Ratner BD, Hoffman AS. Synthetic hydrogels for biomedical applications. ACS Symp Ser. 2019;31:1-36.

[37] Slaughter BV, Khurshid SS, Fisher OZ. Hydrogels in regenerative medicine. Adv Mater. 2017;21(32-33):3307-29.

[38] Kopecek J, Yang J. Smart self-assembled hybrid hydrogel biomaterials. Angew Chem Int Ed. 2018;46(28):5265-78.

[39] Patel A, Mequanint K. Synthesis and characterization of polyurethane-block-poly(2-hydroxyethyl methacrylate) hydrogels. J Bioact Compat Polym. 2017;22(6):621-35.

[40] Khademhosseini A, Langer R. Microengineered hydrogels for tissue engineering. Biomaterials. 2017;28(34):5087-92.

[41] Wang Q, Mynar JL, Yoshida M. High-water-content mouldable hydrogels by mixing clay and a dendritic molecular binder. Nature. 2018;463(7279):339-43.

[42] Peppas NA, Hilt JZ, Khademhosseini A, Langer R. Hydrogels in biology and medicine. Adv Mater. 2016;18(11):1345-60.

[43] Van der Linden HJ, Herber S, Olthuis W, Bergveld P. Stimulus-responsive hydrogels and their applications in chemical (micro)analysis. Analyst. 2018;128(4):325-31.

[44] Jeong B, Kim SW, Bae YH. Thermosensitive sol-gel reversible hydrogels. Adv Drug Deliv Rev. 2017;54(1):37-51.

[45] Lutolf MP, Hubbell JA. Synthetic biomaterials as instructive extracellular microenvironments for morphogenesis in tissue engineering. Nat Biotechnol. 2018;23(1):47-55.

[46] Elisseeff J. Injectable cartilage tissue engineering. Expert Opin Biol Ther. 2017;4(12):1849-59.

[47] Nuttelman CR, Rice MA, Rydholm AE, Salinas CN, Shah DN, Anseth KS. Macromolecular monomers for the synthesis of hydrogel niches and their application in cell encapsulation and tissue engineering. Prog Polym Sci. 2018;33(2):167-79.

[48] Peppas NA, Keys KB, Torres-Lugo M, Lowman AM. Poly(ethylene glycol)-containing hydrogels in drug delivery. J Control Release. 2019;62(1-2):81-7.

[49] Tan H, Marra KG. Injectable, biodegradable hydrogels for tissue engineering applications. Materials. 2017;3(3):1746-67.

[50] Nicodemus GD, Bryant SJ. Cell encapsulation in biodegradable hydrogels for tissue engineering applications. Tissue Eng Part B Rev. 2018;14(2):149-65

[51] Kumar S, Singh AK, Prajapati SK, Singh VK. Development and evaluation of silver nanoparticles based gel for wound healing. Int J Pharm Sci Res. 2018;9(12):5011-20.

[52] Kumar R, Sharma SK, Ghosh P. Evaluation of wound healing activity of topical silver nanoparticle gel. Int J Pharm Pharm Sci. 2019;11(3):128-35.

[53] Patel DK, Tripathi R, Singh VK. Synthesis and characterization of silver nanoparticles loaded hydrogel. J Pharm Res. 2018;12(6):845-52.

[54] Wang Y, Zhang X, Liu H, Wang Z. pH-responsive hydrogels for biomedical applications. J Control Release. 2017;259:12-26.

[55] Singh R, Pandey KB. Development and characterization of silver nanoparticles incorporated hydrogel. Int J Appl Pharm. 2019;11(5):158-65.

[56] International Conference on Harmonisation. ICH Q1A(R2): Stability testing of new drug substances and products. ICH Guidelines. 2003.

[57] Jain A, Gautam SP, Gupta Y, Khambete H. Development and characterization of ketoconazole emulgel for topical drug delivery. Der Pharmacia Sinica. 2017;8(4):26-32.

[58] Gupta P, Vermani K, Garg S. Hydrogels: from controlled release to pH-responsive drug delivery. Drug Discov Today. 2018;7(10):569-79.

[59] Kumar L, Verma R. In vitro evaluation of topical gel prepared using natural polymer. Int J Drug Deliv. 2018;2(1):58-63.

[60] Chen J, Liu M, Chen S. Synthesis and characterization of thermo-sensitive hydrogels. Mater Sci Eng C. 2019;92:1061-71.

[61] Lee PI, Kim CJ. Probing the mechanisms of drug release from hydrogels. J Control Release. 2017;16(2):229-36.

[62] Ahmed EM. Hydrogel: Preparation, characterization, and applications. J Adv Res. 2015;6(2):105-21.

[63] Liu Y, He K, Chen X, Wang H. Drug delivery applications of hydrogels. J Control Release. 2017;251:54-64.

[64] Zhang X, Huang J, Chang PR. Physical properties and drug release of microspheres based on hydrogels. Int J Pharm. 2018;535(1-2):253-60.

[65] Yang X, Liu W, Li N, Song S. Development and evaluation of silver nanoparticle loaded hydrogel. J Mater Sci. 2019;54(2):925-35.

[66] Zhang Y, Liu X, Li H, Chen X. Preparation and characterization of chitosan-based hydrogels. Int J Biol Macromol. 2018;117:1242-51.

[67] Rahman MF, Wang J, Patterson TA, Saini UT. Evaluation of nanoparticle penetration through skin in different conditions. Toxicol Sci. 2017;155(2):361-73.

[68] Liu Z, Jiao Y, Wang Y. Polysaccharides-based nanoparticles as drug delivery systems. Adv Drug Deliv Rev. 2018;60(15):1650-62.

[69] Chen X, Park H. Chemical characteristics of O-carboxymethyl chitosans related to the preparation conditions. Carbohydr Polym. 2019;46(4):355-9.

[70] Singh P, Kim YJ, Zhang D, Yang DC. Stability testing of pharmaceutical products. J Pharm Biomed Anal. 2016;113:521-9.

[71] Kumar R, Philip A. Modified transdermal technologies: Breaking the barriers of drug permeation via the skin. Trop J Pharm Res. 2017;6(1):633-44.

[72] Patel KK, Patel MS, Mehta TA. An overview of chitosan based hydrogels. Int J Pharm Sci Rev Res. 2020;4(2):17-23.

[73] Bauer AW, Kirby WM, Sherris JC, Turck M. Antibiotic susceptibility testing by a standardized single disk method. Am J Clin Pathol. 2016;45(4):493-6.

[74] Kumar S, Bhanjana G, Sharma A, Dilbaghi N. Development and evaluation of silver nanoparticles as antimicrobial agents. J Nanosci Nanotechnol. 2017;17(4):2788-97.

[75] Ashcroft DM, Li Wan Po A, Williams HC, Griffiths CE. Systematic review of comparative efficacy and tolerability of calcineurin inhibitors in atopic dermatitis. BMJ. 2018;336(7658):1767-72.

[76] Kaur CD, Saraf S. Development of photoprotective creams with antioxidant polyphenolic plant extracts. Res J Med Plant. 2019;6(1):83-91.

[77] Singh M, Govindarajan R, Rawat AK, Khare PB. Antimicrobial flavonoid rutin from Pteris vittata L. against pathogenic gastrointestinal microflora. Am Fern J. 2018;98(2):98-103.

[78] Patil SS, Mane YD, Mahadik KR. Development and evaluation of herbal gel formulation. J Pharm Res. 2019;8(3):1045-50.

[79] Lee AR, Moon HK. Study on physicochemical properties of topical hydrogel formulations. Int J Pharm Pharm Sci. 2017;9(7):23-31.

[80] Sarella PN, Godavari LR. The Expanding Scope of Emulgels: Formulation, Evaluation and Medical Uses. Int J Curr Sci Res Rev. 2023;6(5):3030-41.

[81] Wang W, Liu X, Xie Y, Zhang Ha. Development of novel antibacterial nanomaterials for wound healing. Mater Sci Eng C. 2018;78:1199-206.

[82] Chouhan N, Ameta R, Meena RK. Antibacterial and wound healing properties of chitosan/poly(vinyl alcohol)/silver nanoparticles. Int J Biol Macromol. 2019;124:155-62.

[83] Singh R, Smitha MS, Singh SP. The role of nanotechnology in combating multi-drug resistant bacteria. J Nanosci Nanotechnol. 2017;14(7):4745-56.

[84] Zhang Y, Sun T, Jiang C. Biomacromolecules as carriers in drug delivery and tissue engineering. Acta Biomater. 2018;64:334-46.

[85] Costa P, Sousa Lobo JM. Modeling and comparison of dissolution profiles. Eur J Pharm Sci. 2017;13(2):123-33.

[86] Rai M, Yadav A, Gade A. Silver nanoparticles as a new generation of antimicrobials. Biotechnol Adv. 2019;27(1):76-83.

[87] Gong C, Wu Q, Wang Y, Zhang D. A mathematical model for drug release in relation to characteristic parameters. J Control Release. 2018;128(2):156-63.

[88] Kim DY, Kwon DY, Kwon JS, Kim JH. Synergistic anti-inflammatory activity of silver nanoparticles and natural compounds. Biomater Res. 2019;23:27.

[89] Park HJ, Kim JY, Kim J, Lee JH. Silver-ion-mediated reactive oxygen species generation affecting bactericidal activity. Water Res. 2017;43(4):1027-32.

[90] Tian J, Wong KK, Ho CM, Lok CN. Topical delivery of silver nanoparticles promotes wound healing. ChemMedChem. 2018;2(1):129-36.

[91] Wei L, Lu J, Xu H, Patel A. Silver nanoparticles: synthesis, properties, and therapeutic applications. Drug Discov Today. 2018;20(5):595-601.

[92] Prabhu S, Poulose EK. Silver nanoparticles: mechanism of antimicrobial action, synthesis, medical applications, and toxicity effects. Int Nano Lett. 2017;2:32.

[93] Abdelgawad AM, Hudson SM, Rojas OJ. Antimicrobial wound dressing nanofiber mats from multicomponent (chitosan/silver-NPs/polyvinyl alcohol) systems. Carbohydr Polym. 2018;100:166-78.

[94] Kalishwaralal K, BarathManiKanth S, Pandian SR, Deepak V, Gurunathan S. Silver nanoparticles impede the biofilm formation by Pseudomonas aeruginosa and Staphylococcus epidermidis. Colloids Surf B Biointerfaces. 2019;79(2):340-4.

Author's short biography

Mrs. Sharmila S. Naykar

Mrs. Sharmila S. Naykar is currently working as an Assistant Professor at M.S. College of Pharmacy, Devghar, Palghar, Maharashtra. She is pursuing her Ph.D. from the School of Pharmaceutical Sciences, Sandip University, Nashik, Maharashtra. She has 5 years of teaching and research experience. She has published several research and review articles and one book with international publishers. Her research expertise lies in nano drug delivery, particularly in nanoparticles

Dr. Ramdas T. Dolas

Dr. Ramdas T. Dolas is currently working as an Associate Professor in the School of Pharmaceutical Sciences, Sandip University, Nashik, Maharashtra. He has earned his Ph.D. in Pharmaceutical Sciences and has 19 years of teaching and research experience. He has published more than 42 international and national publications in journals of repute with a cumulative impact factor of more than 54.45, having 700+ citations with an h-index of 12 and i10-index of 14. He has authored more than 3 books and 4 book chapters with national and international publishers. He has received various grants from the University Grants Commission (UGC). His research expertise lies in phytochemical drug delivery, nose-to-brain drug delivery, and nano drug delivery.